CHEMISTRY
A EUROPEAN JOURNAL

DOI: 10.1002/chem.200800075

Size- and Structure-Selective Noncovalent Recognition of Saccharides by Tetraethyl and Tetraphenyl Resorcinarenes in the Gas Phase

Elina Kalenius,*[a] Timo Kekäläinen,[a] Raisa Neitola,[a] Kodiah Beyeh,[b] Kari Rissanen,[b] and Pirjo Vainiotalo[a]

Abstract: The noncovalent complexation of tetraethyl and tetraphenyl resorcinarenes with mono-, di-, and oligosaccharides was studied with negative-polarization electrospray ionization quadrupole ion trap and electrospray ionization Fourier-transform ion cyclotron resonance mass-spectrometric analysis. The saccharides formed 1:1 complexes with deprotonated resorcinarenes, which exhibited clear size and structure selectivity in their complexation. In the case of the monosaccharides, hexoses formed much more abundant and kinetically stable complexes than pentoses or deoxyhexoses. A comparison of the mono-, di-, and oligosaccharides revealed that both the relative abundance and stability of the complexes increase up to biose and triose, but start to decrease after that point, as the length of the oligosaccharide is increased. This behavior was rationalized by comparing the lowest-energy conformations of the complexes formed between the resorcinarene and oligosaccharides. This comparison was achieved by using theoretical calculations and X-ray crystal studies.

Keywords: ab initio calculations · calixarenes · carbohydrates · host–guest chemistry · mass spectrometry

Introduction

The selective and sensitive recognition of saccharides is of infinite importance, not only for medical diagnostics and industrial processes, but also for the food industry. Saccharides play a key role in many biochemical series of events, such as the energy balance of organisms, intercellular communication, and cellular and molecular targeting.[1] The development of a fast and efficient detection methodology would allow an immediate perception of alterations caused by disease or medical treatment in the metabolism of organisms. In addition, an effective detection methodology would aid the monitoring of industrial processes, such as fermentation. However, saccharides are an extremely challenging class of compound for selective detection because they are structurally relatively similar, but still have small yet significant differences in their stereochemistry and configuration.[2,3]

At the level of small configurational differences in sugars, separation methods based on molecular recognition have been explored as a solution to their analytical separation.[4] Over the past decade, resorcinarene structures have turned out to be a versatile basis for molecular recognition.[5] Various resorcinarenes have reportedly formed noncovalent and mainly hydrogen-bonded complexes, especially with small polar organic molecules containing nitrogen or oxygen atoms.[6–8]

The saccharide and alkyl glycoside complexation of upper-rim unsubstituted resorcinarenes were earlier studied by Aoyama et al.[9,10] They detected sugar complexes mainly from apolar organic solutions by using circular dichroism (CD) and ^{1}H NMR spectroscopic techniques. In their studies, the extraction of ribose from a polar protic solvent into an apolar aprotic solvent was even reported. According to their observations, unsubstituted resorcinarenes are promising hosts for sugar complexation, and this complexation is mainly based on hydrogen-bonding interactions between the HO sphere of the resorcinarene and the OH groups of the sugars.

Herein, we report a mass-spectrometric study of resorcinarene–sugar complexation. Our goal was to clarify the ef-

[a] Dr. E. Kalenius, T. Kekäläinen, Dr. R. Neitola, Prof. P. Vainiotalo
Department of Chemistry, University of Joensuu
P.O. Box 111, 80101 Joensuu (Finland)
Fax: (+358) 13-251-3360
E-mail: Elina.Kalenius@joensuu.fi

[b] K. Beyeh, Prof. K. Rissanen
Nanoscience Center
Department of Chemistry, University of Jyväskylä
P.O. Box 35, 40014 Jyväskylä (Finland)

Supporting information for this article is available on the WWW under http://www.chemeurj.org/ or from the author.

fects of the configuration of the sugar ring and the size of the sugar. The experimental work was mainly conducted with electrospray ionization quadrupole ion trap (ESI-QIT) and electrospray ionization Fourier-transform ion cyclotron resonance (ESI-FTICR) mass spectrometry. The experimental observations were supported by theoretical ab initio calculations. A crystallization experiment from a 1:1 mixture of ethyl resorcinarene (**1**) and cellobiose (Glc_2) from alcohol–water mixtures was performed to obtain crystalline saccharide–resorcinarene complexes. Surprisingly, only the guest cellobiose crystallized, thus its X-ray structure was obtained. In addition, we were interested in exploring the complexation of di- and oligosaccharides, which has not been a subject of earlier research. Deprotonated tetraethyl and tetraphenyl resorcinarenes were used as potential sugar receptors. Tetraethyl resorcinarene (**1**) adopts a crown (C_{4v}) conformation, which is stabilized by intramolecular hydrogen bonding. However, tetraphenyl resorcinarene (**2**) reportedly adopts either the crown (C_{4v}) or boat (C_{2v}) conformation. The ratio C_{4v}/C_{2v} varies mainly according to reaction time, and longer reaction times favor the formation of a C_{4v} product.[11] Herein, we were interested in studying the effect of the conformation of resorcinarene on its complexation behavior.

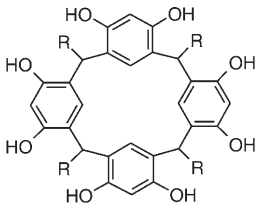

1 R = Et
2 R = Ph

It has been shown that the deprotonation of resorcinarene facilitates the complexation process as a result of a more electron-rich and less hydrophopic cavity, which could lead to better sugar–host CH–π interactions.[12] Therefore, the ability of deprotonated resorcinarenes to complex six different monosaccharides, one disaccharide, and four oligosaccharides (Scheme 1) was studied. Initially, it was our intention to also study tetraethyl pyrogallarene, but the deprotonation of pyrogallarane proved so difficult that this goal had to be reconsidered. In fact, despite numerous attempts in different solution and experimental environments, the pyrogallarane did not produce any peaks for the negative polarization. Even the addition of numerous strong bases was not able to deprotonate the pyrogallarane unit. This outcome is most likely to be the result of a presumably strong intramolecular hydrogen-bonding system formed by the 12 hydroxy groups at the upper rim of the pyrogallarene, which, in fact, is a rather interesting issue.

Our intention was to survey several aspects of the structural properties of saccharides and their effect on the complexation process. The selection of the monosaccharides consisted of three groups of saccharides: pentoses (xylose (Xyl), ribose (Rib)), deoxyhexoses (fucose (Fuc), quinovose (Qui)), and hexoses (galactose (Gal), mannose (Man), glucose (Glu)). In the case of the di- and oligosaccharides, cellosaccharides of increasing length were included (cellobiose (Glc_2), cellotriose (Glc_3), cellotetraose (Glc_4), cellopentaose (Glc_5), cellohexaose (Glc_6)).

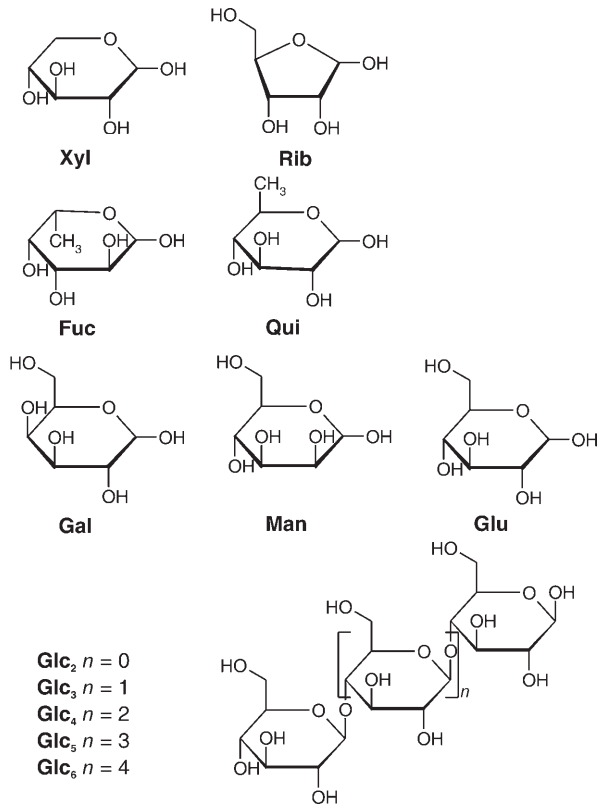

Scheme 1. The mono-, di-, and oligosaccharides studied.

The development of mass spectrometers over recent decades now allows routine the sensitive and nondestructive detection of fragile noncovalent complexes. Therefore, mass spectrometry has become a valuable tool for the characterization of positively charged supramolecular assemblies. However, negative-ionization mass spectrometry has not been used to study noncovalent complexation, although in many cases the experiments would be well suited for negative polarization and the results obtained would create a clearer vision of the interactions involved. Therefore, we were interested in investigating the special characteristics of the negative-mode mass-spectrometric analysis of noncovalent supramolecular complexes.

Results and Discussion

Complex formation with monosaccharides: The spectra recorded from samples containing resorcinarenes **1** or **2** and a single monosaccharide were measured by using both ESI-QIT and ESI-FTICR. There were no significant differences in the appearance of the spectra between these two instruments. In most of the spectra, the peak corresponding to the deprotonated resorcinarene $[M-H]^-$ was observed as the most abundant peak (Figure 1). In addition, the resorcinarenes formed deprotonated ions that corresponded with $[M-2H]^{2-}$ and $[2M-H]^-$. The singly charged complexes with monosaccharides $[M-H+\text{monosaccharide}]^-$ were ob-

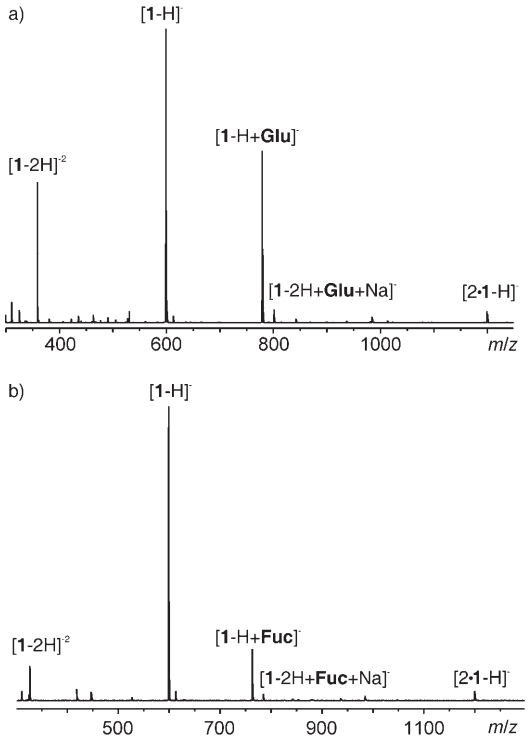

Figure 1. ESI-FTICR spectra measured from samples containing a) **1** and Glu and b) **1** and Fuc in ratios of 1:5 in MeOH

served with every monosaccharide, although the absolute intensities of the ions corresponding to complexes varied per monosaccharide. Clearly, the most abundant complexes were formed with hexoses and the intensity of the peaks was lowest with pentoses.

Furthermore, a peak corresponding to $[M-2H+\text{monosaccharide}+Na]^-$ was generally observed (Figure 1). This ion is most likely the result of a replacement of a $-OH$ hydrogen atom of the resorcinarene with a sodium cation. A cross-check by using positive polarization also showed an abundant formation of sodium adducts $[\text{monosaccharide}+Na]^+$ and $[M+Na+\text{monosaccharide}]^+$. Occasionally, a concentration-dependent clustering of monosaccharides, such as $[2\times \text{monosaccharide}-H]^-$, was also observed. Most likely, this behavior does not have a specific nature, but since no further investigations were made on that issue, the nature of these ions remains uncertain.

In the case of monosaccharides, there were no signs of an association with resorcinarene dimers or the formation of complexes that consisted of several monosaccharides and resorcinarene, although the observation of such complexes have been previously reported.[10]

The relative affinity of resorcinarenes towards saccharides was studied in a bilaterally competitive environment. In these experiments, each sample contained 1:3:3 of each resorcinarene and two competitive monosaccharides. In the case of di- and oligosaccharides, a host/guest$_1$/guest$_2$ ratio of 1:1:1 was used to decrease sugar clustering. An ESI-QIT instrument was used to record the competition experiments.

The monosaccharide competition experiments of resorcinarene **1** were mainly performed against Fuc, and all the studied monosaccharides were included in the experiments. Additionally, a competition experiment was also performed between Qui and Glu to achieve a comparison between Fuc and Qui. The results from the competitive complexation experiments for **1** and monosaccharides are presented in Figure 2.

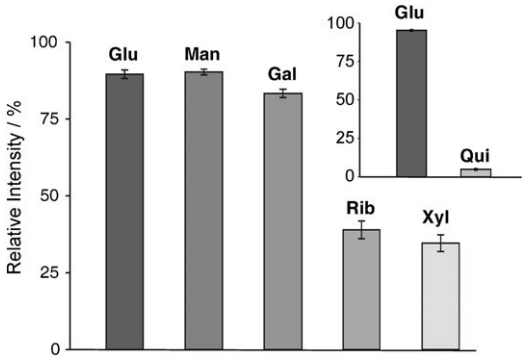

Figure 2. Relative intensities (%) of monosaccharide complexes ($[\mathbf{1}+\text{saccharide}-H]^-/[\mathbf{1}+\text{saccharide}-H]^-+[\mathbf{1}+\text{Fuc}-H]^-$) and the relative intensities (%) of Glu and Qui (upper right).

The results clearly confirm earlier observations: the ion abundances of the complexes of hexoses with resorcinarene **1** are higher relative to the pentoses and deoxyhexoses. Among the hexoses, Gal seems to form a slightly less abundant complex than Glu and Man. Moreover, Fuc forms a slightly more abundant complex than Qui. Overall, the affinity of resorcinarene **1** can be given in the following decreasing order: $\text{Glu}\approx\text{Man}>\text{Gal}\gg\text{Fuc}>\text{Rib}\approx\text{Xyl}$. Whether the complexation efficiency of Qui is higher than the efficiency of pentoses cannot be concluded from these results.

The monosaccharide competition experiments in the presence of resorcinarene **2** were performed only with the pairs Glu/Fuc, Xyl/Fuc, and Glu/Qui (Figure 3). Similarly, as with resorcinarene **1**, the affinity of resorcinarene **2** decreases in the order: $\text{Glu}\gg\text{Fuc}\approx\text{Xyl}$.

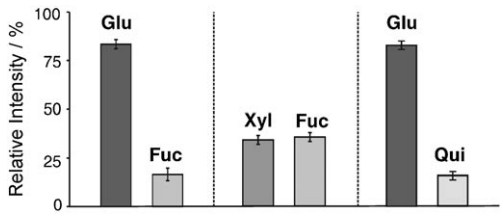

Figure 3. Monosaccharide competitions in the presence of **2**. The relative intensities (%) are presented.

Complex formation with di- and oligosaccharides: It was also observed that all of the di- and oligosaccharides com-

plex with both resorcinarenes. According to the spectra, the most abundant ions were formed from the complexes with cellobiose and -triose. In the spectra of a sample with a host/guest ratio of 1:5, more intense peaks corresponding to saccharide clusters were observed relative to the monosaccharides. Therefore, a resorcinarene/saccharide ratio of 1:1 was used in further measurements of the di- and oligosaccharide complexes. The peaks that corresponded to the deprotonated di- and oligosaccharides were also much more intense relative to the monosaccharides. Occasionally, doubly charged complexes, such as $[2M+\text{saccharide}-2\text{H}]^{2-}$, $[M+2\times\text{saccharide}-2\text{H}]^{2-}$, and $[M+\text{saccharide}-2\text{H}]^{2-}$, were also observed, but the intensity was relatively low. It might be possible, though, for di- and oligosaccharides to form multiply charged complexes with the resorcinarene dimer as a result of better stabilization of the multiple charges.

Competitive complexation experiments were performed for di- and oligosaccharides in the presence of resorcinarenes (Figure 4). Our interest was mainly focused on the possible complexation size selectivity of resorcinarenes and the difference in size selectivity between the two resorcinarenes. As a result of high (or big) mass differences between the di- and oligosaccharides, the competition experiments were performed bilaterally by using the competition pairs Glu/Glc_2, Glc_2/Glc_3, Glc_3/Glc_4, Glc_4/Glc_5, and Glc_5/Glc_6. For each competition pair, the experimental parameters were optimized for the lower-mass complex, which might, therefore, be slightly overestimated. Resorcinarene **1** exhibited size selectivity towards Glc_3, and the size selectivity of resorcinarene **1** is $Glu < Glc_2 < Glc_3 > Glc_4 > Glc_5 > Glc_6$.

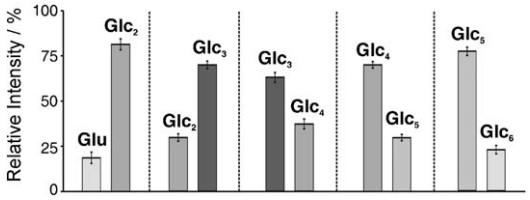

Figure 4. Di- and oligosaccharide competitions in the presence of **1**. The relative intensities (%) are presented.

A similar size-selectivity order is observed for resorcinarene **2** (Figure 5). According to earlier studies, the differences in resorcinarene conformation also induce clear differences in their complexation behavior. It was observed that boat conformers prefer to complex with elongated ammonium ions, whereas the crown conformers prefer small and branched ammonium ions.[13] Herein, resorcinarenes **1** and **2** did not show any difference in their complexation of di- and oligosaccharides. Therefore, it seems rather clear that in these experiments both the resorcinarenes have adopted a similar conformation, despite the earlier assumption.

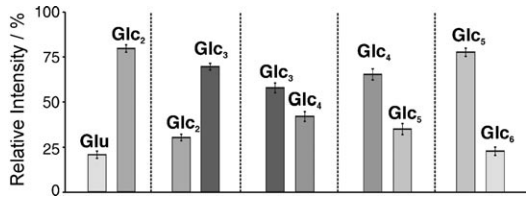

Figure 5. Di- and oligosaccharide competitions in the presence of **2**. The relative intensities (%) are presented.

Theoretical calculations and X-ray structure studies of cellobiose: The complex formation with large oligosaccharides, such as cellopentaose and cellohexaose, was a rather surprising observation. Although, other complexes of resorcinarene have previously been modeled,[14] to the best of our knowledge complexes with sugars have not been reported, and so we were constrained to looking more closely at the conformation of the oligosaccharides by using theoretical calculations. In the first stage, the structures of Glu, Glc_2, Glc_3, Glc_4, and Glc_5 were optimized (Figure 6).

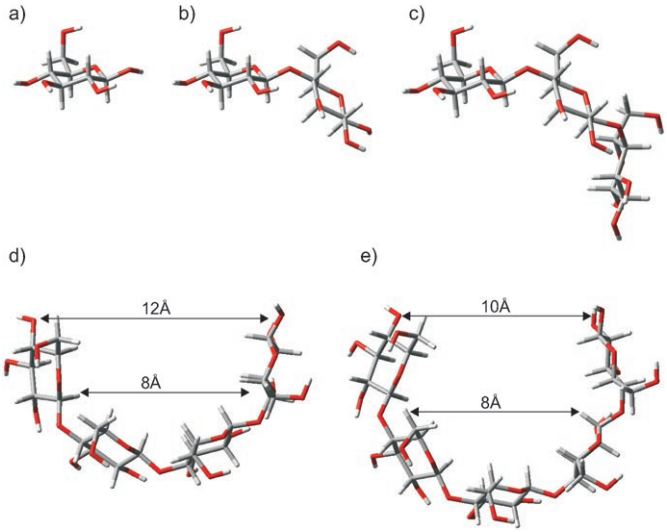

Figure 6. The lowest-energy conformations of saccharides: a) glucose (Glu), b) cellobiose (Glc_2), c) cellotriose (Glc_3), d) cellotetraose (Glc_4), and e) cellopentaose (Glc_5).

The conformations presented in Figure 6 were obtained at the BP86/SVP level of theory. The lowest-energy form of glucose possessed a six-membered ring (chair conformation) and a counter-clockwise network of intramolecular hydrogen bonds. The lowest-energy conformation of cellobiose was compared to its X-ray crystal structure (Figure 7). Attempts to crystallize **1** with excess cellobiose from a PrOH/H_2O mixture did not make the complex visible in the gas state. The difference in solubility of the components, namely, **1** is not soluble in water and cellobiose is only soluble in water, is the probable cause of the negative result. However, to our surprise, the cellobiose itself formed a crystal under these conditions that was of sufficient quality for X-ray diffraction studies. The structure of the cellobiose in its solid state differs from the modeling in the configuration of the bridge-head methine hydrogen atoms. In the crystals,

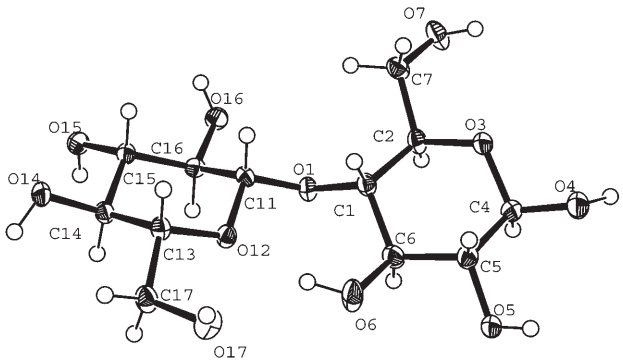

Figure 7. A plot of cellobiose with atom labels. The thermal displacement parameters are shown at a 50% probability level.

they have a *cis* configuration (Figure 7) and result in a flat overall structure (Figure 8a). The governing factor for the flat *cis* configuration is the formation of fairly strong intra-

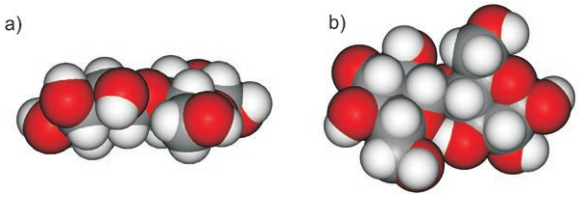

Figure 8. The CPK presentations of cellobiose: a) side and b) top views.

molecular hydrogen bonds between O(6) and O(12) (Figure 7 and 8b) and O(6)-H···O(12) and O(6)···O(12) with distances of 1.951 and 2.768 Å, respectively, and with an O–H···O angle of 164.03°.

The calculated energy of the crystal structure is close to the optimized lowest-energy conformation of cellobiose. However, the difference in these energies indicates that the crystal structure differs from the theoretically calculated structure of cellobiose. The full geometry optimized structure of cellobiose is not as linear as the geometry in the crystal structure because of the different position of the hydroxymethyl groups.[15] Furthermore, a clear curvature of the saccharide skeleton is evident as the number of glucose residues exceeds two (the oligosaccharides larger than Glc_2).[16] The curvature of the oligosaccharide skeleton decreases the length of the saccharide to 10–12 Å (Figure 6), which corresponds to the diameter of the upper rim of the resorcinarenes (≈10 Å), as approximated from the optimized structure of **1**.

In the next stage, the complexes of **1** with glucose, cellobiose, and cellotriose were optimized by using the density functions BP86 and B3LYP, both with a SVP basis set. The lowest-energy conformations of the host–guest complexes are presented in Figure 9. Optimized structures **1a** and **1b** are the two most stable geometries for the complex formed with glucose. The calculated total energy difference between those two cases is only 20 kJ mol^{-1} (Table 1). Still, the differ-

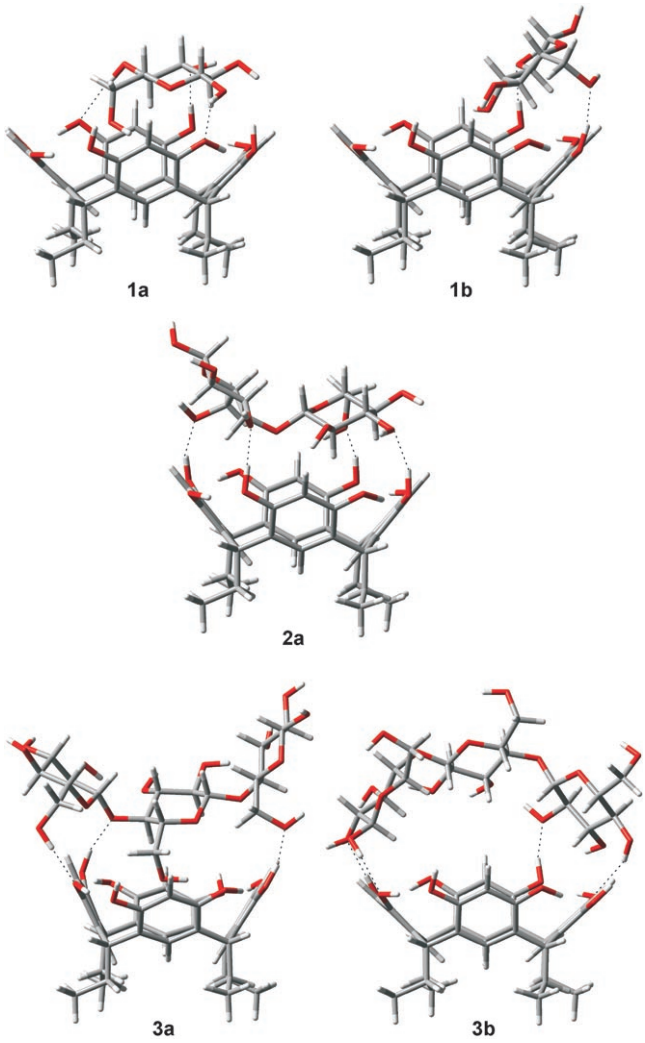

Figure 9. The optimized structures for host–guest complexes of **1** calculated by using the BP86/SVP method: **1a** and **1b** with Glu, **2a** with Glc_2, and **3a** and **3b** with Glc_3.

ences in the position of glucose are obvious. In **1a**, the glucose molecule lies on the top of the upper rim of the resorcinarene and the hydroxymethyl group points towards the middle of the cavity. Furthermore, a conformational change occurs and the crown conformation of the resorcinarene is slightly flattened and the cavity becomes more oval. This result is most likely because of a repulsion between the hydroxymethyl oxygen atom of the glucose and the aromatic rings of the resorcinarene. In **1b**, the glucose molecule is situated on one side of the cavity and is lifted so that the hydroxymethyl group is positioned along the edge of the upper rim of the resorcinarene. This position allows the formation of two hydrogen bonds. Even though there are three hydrogen bonds in **1a** and only two in **1b**, the interaction energy of **1b** is 20 kJ mol^{-1} lower than the interaction energy in **1a**. Probably, the repulsion interaction in geometry **1a** is the main reason for its decreased interaction energy, as calculated by the density-functional method. In addition to hydrogen bonding such interactions as van der

Table 1. Calculated total and interaction energies of the complexes of **1** formed with glucose, cellobiose, and cellotriose obtained by using BP86/SVP, B3LYP/SVP, and MP2/TZVP levels of theory.

Complex	Method	Total energy [a.u.]	$\Delta E^{[a]}$ [kJ mol^{-1}]
1a **1**+Glu	BP86/SVP	−2683.1728	−63
1a **1**+Glu	B3LYP/SVP	−2681.4744	−68
1a **1**+Glu	MP2/TZVP	−2678.4961	−121
1b **1**+Glu	BP86/SVP	−2683.1809	−84
1b **1**+Glu	B3LYP/SVP	−2681.4801	−83
1b **1**+Glu	MP2/TZVP	−2678.4955	−119
2a **1**+Glc_2	BP86/SVP	−3293.5388	−109
2a **1**+Glc_2	B3LYP/SVP	−3291.4783	−115
2a **1**+Glc_2	MP2/TZVP	−3287.9057	−158
3a **1**+Glc_3	BP86/SVP	−3903.8740	−73
3a **1**+Glc_3	B3LYP/SVP	−3901.4541	−87
3a **1**+Glc_3	MP2/TZVP	−3897.3043	−165
3b **1**+Glc_3	BP86/SVP	−3903.8822	−95
3b **1**+Glc_3	B3LYP/SVP	−3901.4585	−98
3b **1**+Glc_3	MP2/TZVP	−3897.2859	−117

[a] Interaction energies.

Waals and CH−π interactions should be taken into account. Therefore, the MP2 energies were calculated from BP86 optimized structures. The MP2 method is computationally very demanding, but it takes more noncovalent interactions into consideration. Therefore, it was not surprising that according to the MP2 method the interactions between host and guest molecules are stronger than those calculated by the density-functional method. It is noteworthy that there was no difference between the interaction energies of **1a** and **1b**, as calculated by using the MP2 method. The interaction energies of the host–guest complexes calculated by using BP86/SVP, B3LYP/SVP and MP2/TZVP are summarized in Table 1.

In Figure 9, **2a** represents the lowest-energy geometry for the cellobiose complex of resorcinarene **1**. The calculated interaction energy of **2a** was lower than that of glucose complexes **1a** and **1b**. In other words, the biose formed a much more stable complex than glucose as a result of the stronger interaction between the host and guest molecules. This result is in agreement with the experimental results obtained from the competition experiments. Visualization of the full geometry optimized structure (Figure 9; **2a**) provides insight into the increased stability of the complex formed between the biose and **1**. Cellobiose is situated in the middle of the resorcinarene and almost completely covers the cavity of the resorcinarene. In addition, the geometry and position of cellobiose enables it to interact with almost the entire upper rim of the resorcinarene. There are four evident hydrogen bonds between the resorcinarene and cellobiose. These hydrogen bonds bind the cellobiose to resorcinarene from both sides of the upper rim. The hydrogen bonds between the cellobiose and resorcinarene are not more than 1.8 Å.

The final objective of the theoretical study was to investigate the interactions between cellotriose and **1**. In Figure 9, the most stable structures for a cellotriose complex of **1** are presented. The position of the saccharide unit differs significantly in the two investigated cases of **3a** and **3b**. In **3a**, the cellotriose lies in the middle of the resorcinarene and one hydroxymethyl group dives into the middle of the cavity. Three hydrogen bonds are formed between **1** and cellotriose, and their lengths varied between 1.7 and 1.9 Å. However, in structure **3b**, the triose bends to follow the edge of the upper rim of the resorcinarene and all the hydroxymethyl groups point upwards. That arrangement enables the triose to form four hydrogen bonds with the host: two for both ends with lengths from 1.8 to 2.0 Å. As in the case of the glucose complexes (i.e., **1a** and **1b**), the BP86 and B3LYP interaction energies of **3a** are slightly weaker when the $-CH_2OH$ group is almost inside the cavity. The number of hydrogen bonds formed supports the results obtained from density-functional calculations. According to the MP2 method, the interactions in the triose complexes are stronger, as observed earlier for glucose and biose, but surprisingly **3a** seemed to be the favorable configuration. Obviously, the DFT and MP2 theories describe the interactions involved in the complexes in a slightly different way. In context with the experimental results, however, the MP2 theory seems to better describe the complexes under investigation herein. Still, independently from the theory used, the results obtained by theoretical calculations predict that the complexation of biose and triose is more favorable than the complexation of the monosaccharides, which is in agreement with the experimental work of this study.

Kinetic stability of the complexes: Energy-resolved collision induced dissociation (CID) experiments were performed on an ESI-FTICR mass spectrometer. These experiments allow the comparison of the relative kinetic stabilities of the complexes to be carried out. To begin with, dissociation routes of deprotonated resorcinarenes were defined to facilitate the interpretation of the CID spectra. For this purpose, an ESI-QIT instrument and multiple-stage mass spectrometry (MS^n) experiments of the fragment ions were used. Mass accuracy, determined for each fragment ion by using ESI-FTICR equipment, varied from 0.3 to 11 ppm.

Deprotonated **1** dissociated by repeatedly losing neutral molecules of 110, 150, and 190 Da (Scheme 2), which correspond to resorcinol and resorcinol with one or two propyl-

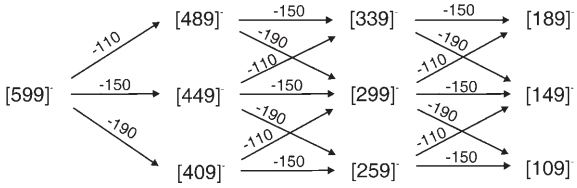

Scheme 2. Dissociation of resorcinarene **1**.

ene chains. In addition, the elimination of water from fragment ions at *m/z* 339 and 299 was weakly observed. The fragment ions formed are highly conjugated, which naturally increases their stability. In the case of resorcinarene **2**, dissociation to similar conjugated structures is not possible as a result of phenyl substituents at the lower rim. Therefore, de-

protonated **2** dissociated through a series of eliminations of resorcinols and water; furthermore, the formation of kinolic fragment ions was mainly observed. The complexes of **1** formed with monosaccharides dissociated and produced deprotonated resorcinarene, which further dissociated to its fragment ions (Figure 10). Deprotonated monosaccharides

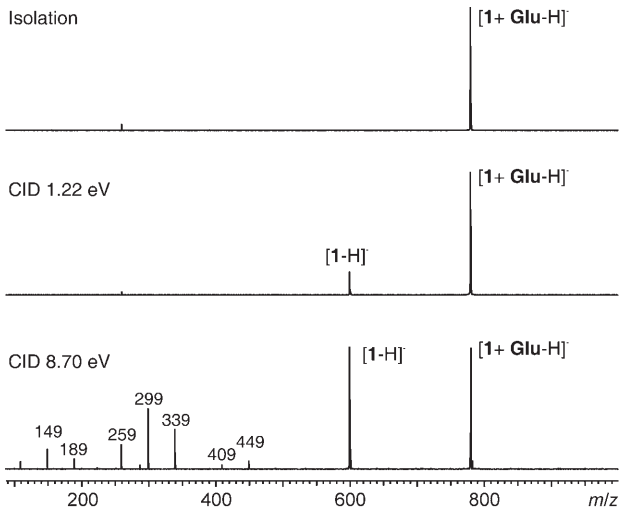

Figure 10. CID of $[\mathbf{1}+\mathrm{Glu}-\mathrm{H}]^-$ complex.

were not observed in any of the CID spectra, thus implying that the complexes are indeed formed from deprotonated resorcinarenes and neutral monosaccharides.

The dissociation of the complexes was followed as a function of energy and the $E_{com}^{0.5}$ values were calculated by using the dissociation curves. The complexes dissociated with relatively low energy values, thus implying that the complexes have low kinetic stabilities. According to the dissociation curves and $E_{com}^{0.5}$ values (Table 2), the most stable monosaccharide complexes were formed with hexoses. The differences in stability were small for the pentoses and deoxyhexoses; therefore, the increasing order of stability for monosaccharide complexes can be written as $\mathrm{Fuc}\approx\mathrm{Rib}\approx\mathrm{Qui}\approx\mathrm{Xyl}<\mathrm{Glu}\approx\mathrm{Gal}<\mathrm{Man}$. Accordingly, kinetic stability increases in the same order as the increase in the affinity of **1** towards monosaccharides.

Similar behavior was also observed with di- and oligosaccharides: the most stable complexes were formed with Glc_2 and Glc_3, which formed the most abundant complexes with **1** in the competition experiments and had the highest interaction energies according to the theoretical calculations. According to these results, the stability follows the order: $\mathrm{Glu}\ll\mathrm{Glc_2}>\mathrm{Glc_3}\gg\mathrm{Glc_4}>\mathrm{Glc_5}>\mathrm{Glc_6}$.

Table 2. Calculated $E_{com}^{0.5}$ values and the correlation R^2 of the dissociation curves.

Complex	$E_{com}^{0.5}$ [eV]	R^2
$[\mathbf{1}+\mathrm{Rib}-\mathrm{H}]^-$	0.87	0.990
$[\mathbf{1}+\mathrm{Xyl}-\mathrm{H}]^-$	0.98	0.993
$[\mathbf{1}+\mathrm{Fuc}-\mathrm{H}]^-$	0.85	0.991
$[\mathbf{1}+\mathrm{Qui}-\mathrm{H}]^-$	0.91	0.985
$[\mathbf{1}+\mathrm{Gal}-\mathrm{H}]^-$	1.35	0.996
$[\mathbf{1}+\mathrm{Man}-\mathrm{H}]^-$	1.60	0.995
$[\mathbf{1}+\mathrm{Glu}-\mathrm{H}]^-$	1.29	0.996
$[\mathbf{1}+\mathrm{Glc_2}-\mathrm{H}]^-$	2.42	0.993
$[\mathbf{1}+\mathrm{Glc_3}-\mathrm{H}]^-$	2.20	0.994
$[\mathbf{1}+\mathrm{Glc_4}-\mathrm{H}]^-$	1.63	0.986
$[\mathbf{1}+\mathrm{Glc_5}-\mathrm{H}]^-$	1.12	0.987
$[\mathbf{1}+\mathrm{Glc_6}-\mathrm{H}]^-$	1.14	0.996

Conclusion

According to this study, deprotonated resorcinarenes **1** and **2** readily form noncovalent 1:1 complexes with neutral saccharides. In addition, these resorcinarenes exhibit a clear structure and size selectivity towards the saccharides. Both the thermodynamic and kinetic stabilities seem to increase with hexoses. This behavior results most likely from a maximum of three hydrogen bonds formed between the hexose and resorcinarene.

According to a comparison of di- and oligosaccharides, it seems that the complexation of biose and triose is the most beneficial and is even more favorable than the binding of a monosaccharide as a result of a maximum of four hydrogen bonds between the host and saccharide. As the sugar chain is increased, the resorcinarene affinity towards saccharides decreases, although the complexation still occurs. It was, unquestionably, a surprise for us that the complexation of such large sugars (i.e., cellohexaose) was observed, but this behavior was rationalized by theoretical calculations that showed the formation of a curved conformation of the larger sugars suitable for interaction with resorcinarenes.

The results partially contradict previously reported observations,[9] although it must be pointed out that the selection of the saccharides, and the methodology used, was quite different in the previous reports relative to the experimental setup presented herein. For these reasons, we will continue our studies of the resorcinarene/saccharide complexes and hopefully will obtain greater insight into the specific interactions involved in these complexes.

The theoretical optimizations of the complexes provided indispensable insight into the complex geometries and interactions involved. Although it was discovered that there are certain marked differences in the levels of theories used: the DFT theory is adequate for describing the geometries of the complexes, but the MP2 theory is preferable for describing the noncovalent interactions involved in the complexes of interest to us. However, MP2 is a rather resource-demanding theory. Therefore, it is reasonable to perform the geometry optimizations by using DFT methods.

As shown herein, negative-ion mass-spectrometric analysis seems to be well suited to the analysis of noncovalent complexes. During the experimental studies, we did not encounter any setbacks. Depending on the investigation and the chemical nature of the supramolecular interacting species, negative-mode mass-spectrometric analysis can, on

many occasions, produce clean spectra and pure interactions, so its use is highly recommended.

Experimental Section

Materials: The synthesis, X-ray structure studies, and characterization of resorcinarene **1** have been reported previously.[17,18] Resorcinarene **2** was prepared according to earlier reported procedures.[14,19] Resorcinarene **1** was dissolved in methanol and resorcinarene **2** in dimethyl sulfoxide (DMSO). The final samples were prepared in methanol with a resorcinarene concentration of 4.0 μM. The saccharides were commercially available. All the monosaccharides were dissolved in methanol. Di- and oligosaccharides were dissolved in H_2O. Molar ratios of 1:1, 1:3, or 1:5 resorcinarene/saccharide were used.

Mass spectrometry: Two separate mass spectrometers were used in this study. The experimental details related to the MS experiments are presented in the Supporting Information. The competition experiments were performed on a Bruker Esquire 3000 plus QIT mass spectrometer (Bruker Daltonik, Bremen Germany) equipped with an ESI source. Each spectrum was an average of spectra collected within 1 min, each of these containing 24 individual scans that were averaged before being sent from the instrument to data system. The mass spectra were externally calibrated with an ES tuning mix (Hewlett Packard, Palo Alto, CA). The competition experiments between the monosaccharides were performed with a resorcinarene/guest$_1$/guest$_2$ ratio of 1:3:3. In the case of the oligosaccharides and disaccharide, a 1:1:1 ratio was used. The competitions were carried out between just two guests at a time to avoid nonspecific complexation, which could arise with a greater number of charged species in solution. Each experiment was carried out on five different samples and each sample was measured five times. The overall variance was calculated from the standard deviation of sampling and the standard deviation of the measurement ($s_{tot}^2 s_1^2 + s_2^2$). Measurements or samples were rejected if the average deviation of a suspect value from the mean was four or more times the average deviation of the retained values. The energy-resolved CID experiments were performed with a BioApex 47e Fourier transform ion cyclotron resonance mass spectrometer equipped with an Infinity cell, a passively shielded 4.7-tesla 160-mm bore superconducting magnet, and an external Apollo electrospray ionization source (Bruker Daltonics, Billerica, MA, USA). In collision-induced dissociation (CID) experiments, precursor ions were isolated twice to achieve a clean isolation by using the correlated harmonic excitation fields (CHEF) procedure.[20] Isolated ions were thermalized during a 3.0-s delay, translationally activated by an on-resonance radio frequency (RF) pulse, and allowed to collide with a pulsed argon background gas. Each spectrum was a collection of 16 scans. Comparable conditions were maintained by keeping the parameters of the pulse program constant.

Computational details: Geometry optimizations of saccharides were carried out with density functional BP86 and hybrid density functional B3LYP. The geometries and relative energies for equilibrium structures obtained with the DFT methods, at low computational expense, have often been in good agreement with experimental values. Herein, the complexation of tetraethyl resorcinarene with different saccharides was investigated by using both the BP86 and B3LYP functionals. Density-functional methods have been shown to be a highly viable method for most organic molecules and large systems consisting of main-group elements. The Karlsruhe split-valence basis set with polarization functions (SVP)[21] was applied to both the DFT methods. In addition to the optimization, the single-point energies were calculated for saccharide complexes of tetraethyl resorcinarene by using the Møller–Plesset (MP) perturbation theory. A second-order Møller–Plesset (MP2) perturbation theory was used to improve the description of the electron correlation and DFT interaction energies. The MP2 calculations were performed by using the resolution of the identity (RI) technique as implemented in TURBOMOLE.[22,23] Single-point MP2 energies were calculated by a triple-valence-zeta basis set with polarization functions (TZVP)[24] at the BP86 optimized structures.

The geometry optimizations and energy calculations were performed with the TURBOMOLE 5.9 Program Package[25] by using the efficient resolution of the identity (RI) technique. The visualization of optimized structures was performed with GausView3.0.[26]

X-ray analysis:[27] Colorless crystals of cellobiose were selected, and analysis was performed by using a Bruker Kappa Apex II diffractometer with graphite-monochromatized $Mo_{K\alpha}$ ($l = 0.71073$ Å) radiation. Collect software[28] was used for the data measurement and DENZO-SMN[29] for the processing. The structures were solved by direct methods with SIR97[30] and refined by full-matrix least-squares methods with the WinGX-software,[31] which utilizes the SHELXL-97 module.[32] All C–H hydrogen positions were calculated using a riding atom model with $U_H = 1.5 \times U_O$. Crystal data for the cellobiose: $M_r = 342.30$, colorless prism, $0.15 \times 0.20 \times 0.20$ mm^3, monoclinic, space group $P2_1$, $a = 5.0633(2)$, $b = 13.0170(5)$, $c = 10.9499(4)$ Å, $b = 90.811(2)°$, $V = 721.62(2)$ Å^3, $Z = 2$, $\rho_{cald} = 1.575$ g cm^{-3}, $F_{000} = 364$, $m = 0.141$ mm^{-1}, $T = 173.0(1)$ K, $2q_{max} = 50.0°$, 2482 reflections, 2328 with $I_o > 2\sigma(I_o)$, 217 parameters, 0 restraints, GoF = 1.049, $R_1 = 0.0391$, $wR_2 = 0.0841$ (all reflections), $0.322 < Dr < -0.199$ e Å^{-3}.

Acknowledgements

The authors gratefully acknowledge financial support from the Magnus Ehrnrooth foundation (E.K., R.N.), the MaBio project of the European Social Fund and the State provincial office of Eastern Finland, the Department of Education and Culture (E.K.), the Academy of Finland (K.R.; prof. no. 122350), and the Graduate School of Organic Chemistry and Chemical Biology (K.B.).

[1] R. A. Dwek, *Chem. Rev.* **1996**, *96*, 683–720.
[2] J. F. Stoddart, *Stereochemistry of Carbohydrates*, Wiley-Interscience, New York, **1971**.
[3] S. J. Angyal, *Angew. Chem.* **1969**, *81*, 172–182; *Angew. Chem. Int. Ed. Engl.* **1969**, *8*, 157–166.
[4] S. H. Gellman, *Chem. Rev.* **1997**, *97*, 1231–1232.
[5] a) H.-J. Schneider, U. Schneider, *J. Inclusion Phenom. Mol. Recognit. Chem.* **1994**, *19*, 67–83; b) P. Timmerman, W. Verboom, D. N. Reinhoudt, *Tetrahedron* **1996**, *52*, 2663–2704; c) B. Botta, M. Cassani, I. D'Acquarica, D. Misiti, D. Subissati, G. Delle Monache, *Curr. Org. Chem.* **2005**, *9*, 337–355; d) B. Botta, M. Cassani, I. D'Acquarica, D. Misiti, D. Subissati, G. Zappia, G. Delle Monache, *Curr. Org. Chem.* **2005**, *9*, 1167–1202; e) A. Shivaniuk, K. Rissanen, E. Kolehmainen, *Chem. Commun.* **2000**, 1107–1108; f) D. Falábu, A. Shivaniuk, M. Nissinen, K. Rissanen, *Org. Lett.* **2002**, *4*, 3019–3022; g) H. Mansikkamäki, M. Nissinen, K. Rissanen, *Chem. Commun.* **2002**, 1902–1903; h) H. Mansikkamäki, M. Nissinen, K. Rissanen, *Angew. Chem. Int. Ed.* **2004**, *43*, 1263–1266; i) H. Mansikkamäki, C. A. Schalley M. Nissinen, K. Rissanen, *New J. Chem.* **2005**, *29,* 116–127; j) M. Vázquez, J. Bobacka, M. Luostarinen, K. Rissanen, A. Lewenstam, A. Ivaska, *J. Solid State Electrochem.* **2005**, *9,* 312–319; k) H. Mansikkamäki, M. Nissinen, K. Rissanen, *CrystEngComm* **2005**, 519–526; l) H. Mansikkamäki, S. Busi, M. Nissinen, A. Åhman, K. Rissanen, *Chem. Eur. J.* **2006**, *12,* 4289–4296; m) N. K. Beyeh, M. Kogej, A. Åhman, K. Rissanen, C. A. Schalley, *Angew. Chem.* **2006**, *118*, 5343; *Angew. Chem. Int. Ed. Angew. Chem. Int. Ed. Engl.* **2006**, *45*, 5214–5218; n) N. K. Beyeh, D. Fehér, M. Luostarinen, C. A. Schalley, K. Rissanen, *J. Inclusion Phenom. Macrocyclic Chem.* **2006**, *54–56*, 381–394; o) N. K. Beyeh, J. Aumanen, A. Åhman, M. Luostarinen, H. Mansikkamäki, M. Nissinen, J. Korppi-Tommola, K. Rissanen, *New J. Chem.* **2007**, *31*, 370–377.
[6] K. Kobayashi, Y. Asakawa, Y. Kikuchi, H. Toi, Y. Aoyama, *J. Am. Chem. Soc.* **1993**, *115*, 2648–2654.
[7] a) H.-J. Schneider, D. Güttes, U. Schneider, *Angew. Chem.* **1986**, *98*, 635–636; *Angew. Chem. Int. Ed. Engl.* **1986**, *25*, 647–649; b) H. Konishi, O. Morikawa, *Chem. Express* **1992**, *7*, 801–804; c) H.-J. Schneider, D. Güttes, U. Schneider, *J. Am. Chem. Soc.* **1988**, *110*, 6449–6454; d) M. Mäkinen, P. Vainiotalo, M. Nissinen, K. Rissanen,

J. Am. Soc. Mass Spectrom. **2003**, *14*, 143–151; e) H. Mansikkamäki, M. Nissinen, C. A. Schalley, K. Rissanen, *New J. Chem.* **2003**, *27*, 88–97; f) E. Ventola, K. Rissanen, P. Vainiotalo, *Chem. Eur. J.* **2004**, *10*, 6152–6162.

[8] a) I. Higler, P. Timmerman, W. Verboom, D. N. Reinhoudt, *J. Org. Chem.* **1996**, *61*, 5920–5931; b) A. Friggeri, F. C. J. M. van Veggel, D. N. Reinhoudt, *Chem. Eur. J.* **1999**, *5*, 3595–3602.

[9] Y. Aoyama, Y. Tanaka, S. Sugahara, *J. Am. Chem. Soc.* **1989**, *111*, 5397–5404.

[10] Y. Kikuchi, Y. Tanaka, S. Sutarto, K. Kobayashi, H. Toi, Y. Aoyama, *J. Am. Chem. Soc.* **1992**, *114*, 10302–10306.

[11] L. M. Tunstad, J. A. Tucker, E. Dalcanale, J. Weiser, J. A. Bryant, J. C. Sherman, R. C. Helgeson, C. B. Knobler, D. J. Cram, *J. Org. Chem.* **1989**, *54*, 1305–1312.

[12] R. Yanagihara, Y. Aoyama, *Tetrahedron Lett.* **1994**, *35*, 9725–9728.

[13] M. Mäkinen, P. Vainiotalo, M. Nissinen, K. Rissanen, *J. Am. Soc. Mass Spectrom.* **2003**, *14*, 143–151.

[14] a) A. B. Rozhenko, W. W. Schoeller, M. C. Letzel, B. Decker, C. Agena, J. Mattay, *THEOCHEM* **2005**, *732*, 7–20; b) A. R. M. Hyyryläinen, J. M. H. Pakarinen, P. Vainiotalo, G. Stájer, F. Fülop, *J. Am. Soc. Mass Spectrom.* **2007**, *18*, 1038–1045.

[15] a) G. L. Strati, J. L. Willett, F. A. Momany, *Carbohydr. Res.* **2002**, *337*, 1833–1849; b) G. L. Strati, J. L. Willett, F. A. Momany, *Carbohydr. Res.* **2002**, *337*, 1851–1859.

[16] I. Sergeyev, G. Moyna, *Carbohydr. Res.* **2005**, *340*, 1165–1174.

[17] H. Erdtman, S. Högberg, S. Abrahamsson, B. Nilsson, *Tetrahedron Lett.* **1968**, 1679–1682.

[18] M. Nissinen, E. Wegelius, D. Falábu, K. Rissanen, *CrystEngComm* **2000**, *28*, 1–3.

[19] A. G. S. Högberg, *J. Am. Chem. Soc.* **1980**, *102*, 6046–6050.

[20] L. J. de Koning, N. M. M. Nibbering, S. L. Van Orden, F. H. Laukien, *Int. J. Mass Spectrom. Ion. Processes*, **1997**, *165/166*, 209–219.

[21] A. Schäfer, H. Horn, R. Ahlrichs, *J. Chem. Phys.* **1992**, *97*, 2571–2577.

[22] F. Weigend, M. Häser, *Theor. Chem. Acc.* **1997**, *97*, 331–340.

[23] F. Weigend, M. Häser, H. Petzelt, R. Ahlrichs, *Chem. Phys. Lett.* **1998**, *294*, 143–152.

[24] A. Schäfer, C. Huber, R. Ahlrichs, *J. Chem. Phys.* **1994**, *100*, 5829–5835.

[25] R. Ahlrichs, M. Bär, M. Häser, H. Horn, C. Kölmel, *Chem. Phys. Lett.* **1989**, *162*, 165–169.

[26] Gaussian 03, M. J. Frisch, G. W. Trucks, H. B. Schlegel, G. E. Scuseria, M. A. Robb, J. R. Cheeseman, J. A. Montgomery, Jr., T. Vreven, K. N. Kudin, J. C. Burant, J. M. Millam, S. S. Iyengar, J. Tomasi, V. Barone, B. Mennucci, M. Cossi, G. Scalmani, N. Rega, G. A. Petersson, H. Nakatsuji, M. Hada, M. Ehara, K. Toyota, R. Fukuda, J. Hasegawa, M. Ishida, T. Nakajima, Y. Honda, O. Kitao, H. Nakai, M. Klene, X. Li, J. E. Knox, H. P. Hratchian, J. B. Cross, V. Bakken, C. Adamo, J. Jaramillo, R. Gomperts, R. E. Stratmann, O. Yazyev, A. J. Austin, R. Cammi, C. Pomelli, J. W. Ochterski, P. Y. Ayala, K. Morokuma, G. A. Voth, P. Salvador, J. J. Dannenberg, V. G. Zakrzewski, S. Dapprich, A. D. Daniels, M. C. Strain, O. Farkas, D. K. Malick, A. D. Rabuck, K. Raghavachari, J. B. Foresman, J. V. Ortiz, Q. Cui, A. G. Baboul, S. Clifford, J. Cioslowski, B. B. Stefanov, G. Liu, A. Liashenko, P. Piskorz, I. Komaromi, R. L. Martin, D. J. Fox, T. Keith, M. A. Al-Laham, C. Y. Peng, A. Nanayakkara, M. Challacombe, P. M. W. Gill, B. Johnson, W. Chen, M. W. Wong, C. Gonzalez, J. A. Pople, Gaussian, Inc., Wallingford CT, **2004**.

[27] CCDC 673203 contains the supplementary crystallographic data for this paper. The data can be obtained free of charge from The Cambridge Crystallographic Data Centre via www.ccdc.cam.ac.uk/data_request/cif.

[28] R. W. Hooft, *COLLECT*, Nonius BV, Delft (The Netherlands) **1998**.

[29] Z. Otwinowski, W. Minor, *Methods Enzymol.***1997**, *276*, 307.

[30] A. Altomare, M. C. Burla, M. Camalli, G. L. Cascarano, C. Giacovazzo, A. Guagliardi, A. G. G. Moliterni, G. Polidori, R. Spagna, *J. Appl. Crystallogr.* **1999**, *32*, 115.

[31] L. J. Farrugia, *J. Appl. Crystallogr.* **1999**, *32*, 837.

[32] G. M. Sheldrick, *SHELXL-97 - A program for the Refinement of Crystal Structures*, University of Göttingen, Germany **1997**, release 97–2.

Received: January 14, 2008
Published online: April 16, 2008

